Letter

Direct observation of the exotic β-γ-α decay mode in the $T_z = -1$ nucleus ^{20}Na

Y. B. Wang,[1,*] J. Su,[2,†] Z. Y. Han,[1] B. Tang,[1] B. Q. Cui,[1] T. Ge,[1] Y. L. Lyu,[1] B. A. Brown,[3,‡] C. X. Yuan,[4] L. H. Chen,[1] Z. Q. Chen,[5] B. Dai,[5] B. Guo,[1] X. Y. Li,[1] Y. J. Li,[1] Z. H. Li,[1] G. Lian,[1] R. G. Ma,[1] T. L. Ma,[1] X. Ma,[1] Y. J. Ma,[1] D. Nan,[1] Y. P. Shen,[1] Y. Su,[1] C. G. Wang,[5] H. Y. Wu,[5] F. R. Xu,[5] S. Q. Yan,[1] S. Zeng,[1] H. Zhang,[1] L. Zhang,[1] Y. Zheng,[1] C. Zhou,[6] Y. L. Dang,[1] G. Y. Fu,[1] Y. F. He,[1] F. L. Liu,[1] D. Wu,[1] T. J. Zhang,[1] and W. P. Liu[1,§]

(BRIF Collaboration)

[1]*China Institute of Atomic Energy, P. O. Box 275(10), Beijing 102413, China*

[2]*College of Nuclear Science and Technology, Beijing Normal University, Beijing 100875, China*

[3]*Department of Physics and Astronomy, and National Superconducting Cyclotron Laboratory, Michigan State University, East Lansing, Michigan 48824-1321, USA*

[4]*Sino-French Institute of Nuclear Engineering and Technology, Sun Yat-Sen University, Zhuhai 519082, China*

[5]*School of Physics, Peking University, Beijing 100871, China*

[6]*School of Nuclear Science and Technology, University of South China, Hengyang 421001, China*

(Received 28 May 2020; revised 5 January 2021; accepted 11 January 2021; published 29 January 2021)

The exotic β-γ-α decay mode of ^{20}Na has been directly observed for the first time in the Day-one experiment at the Beijing Radioactive Ion-beam Facility. The ^{20}Na source was produced by using a 100-MeV proton beam bombarding a stack of microporous MgO thick target and delivered as an intense mass separated beam after online ionization. A high-efficiency simultaneous measurement of β, γ, and α transitions enables the β-delayed γ-γ and α-γ coincidence spectroscopy. Three β-γ-α exotic decay sequences in ^{20}Na are discovered, which expands the rare decay modes observed in β decay. Moreover, a β-α–decay sequence to the 6130-keV 3^- state of ^{16}O is observed, which is likely through the 12 367-keV 1^+ state in ^{20}Ne. The experimentally deduced $B(F)$ and $B(GT)$ are compared to the shell-model calculation, the allowed β transition strengths can be well accounted for by using *sd* shell-model space interactions.

DOI: 10.1103/PhysRevC.103.L011301

The atomic nucleus is a quantum many-body system in which a finite number of protons and neutrons are bound together by the strong nuclear interaction. The stability of nucleus against spontaneous decay is related to the proton-to-neutron ratio or in terms of the projection of isospin $T_z = (N - Z)/2$, where N is the number of neutrons and Z the number of protons. Light nuclei up to ^{40}Ca with $T_z = 0$ are mostly stable with large natural abundances, the so-called proton- and neutron-rich isotopes with larger $|T_z|$ values are subject to different decays. β decay is the most common radioactivity, which provides fundamental information on unstable nuclei for our understanding of nuclear structure [1,2] and nuclear astrophysics [3]. Unusual decay modes appear as a result of weakening binding energy, such as the ground state proton [4,5] and two-proton radioactivities [6,7] in nuclei at the proton drip line, such processes also occur via highly excited states of daughter nuclei [8–10]. These constitute the family of known exotic decay modes as highlighted in recent review articles of radioactive decays [11–13].

β decay takes place between isobaric nuclei and proceeds mainly through the allowed Fermi and Gamow-Teller (GT) transitions to the daughter nucleus. In isobaric nuclei, states with the same isospin T and spin-parity J^π form an isobaric multiplet. Fermi transitions occur between the ground state of the parent nucleus and its isobaric analog state (IAS) in the daughter nucleus, thus is useful for testing the validation of the isobaric multiplet mass equation [14]. For nuclei with IAS above the particle threshold, the emission of particles from the IAS is usually sensitive to the isospin mixing. This provides opportunity for exotic decay mode, particle emission from unbound levels may be partially or even totally due to the feeding of γ transitions from the IAS. To date, exotic β-γ-p decay modes have been observed in $T_z = -2$ nuclei ^{32}Ar [15] and ^{56}Zn [16], significant corrections to both $B(F)$ and $B(GT)$ are introduced that demonstrate the importance of the often omitted indirect feeding by γ transitions to the particle intensity. In this paper, we report the first direct observation of exotic β-γ-α decay in $T_z = -1$ nucleus ^{20}Na.

Prior to the present work, many experimental investigations have been carried out for the decay of ^{20}Na through β-delayed α [17–19], β-delayed γ [20], and β-ν angular correlation [21–23], which lead to detailed information on ^{20}Na decay [24]. More than 10 β-delayed α particle lines are known summing to a total α-emission probability of about 20%. Despite many efforts, the α particle lines below 1 MeV first

*ybwang@ciae.ac.cn
†sujun@bnu.edu.cn
‡brown@nscl.msu.edu
§wpliu@ciae.ac.cn

predicted by Pearson *et al.* [25] were only recently realized by an elaborately designed α-^{16}O coincidence experiment at IGISOL facility [26]. Two new α particle lines below 1 MeV were identified and assigned to the known 3^- state at 5621 keV and the 1^- state at 5788 keV in ^{20}Ne, respectively. Based on these new α particle lines, exotic β-γ-α sequences were suggested, including the one from the IAS at 10 277 keV to the 5621 keV 3^- state in ^{20}Ne [26]. Since only the ^{20}Ne resonance states with natural parity can decay directly to the ground state of ^{16}O via α particle emission, the 1^+ and 3^+ states in ^{20}Ne populated by GT transitions may also have exotic γ-α branches. Such β-γ-α sequences are essential in determining the direct β feedings to the low-lying α emitting states in ^{20}Ne. For this purpose, a direct measurement of exotic β-γ-α decay sequences in ^{20}Na has been performed by using a high-intensity pure ^{20}Na beam and the α-γ coincidence spectroscopy.

The experiment was carried out at the Beijing Radioactive Ion-beam Facility (BRIF) [27], which was recently commissioned to provide postaccelerated radioactive ion beams at the Beijing HI-13 Tandem accelerator laboratory. At BRIF, a newly built 100-MeV 200-μA proton cyclotron (CYCIAE-100) [28] serves as the driving accelerator. Reaction products diffusing out of the thick target are ionized by an ion source and separated by a two-stage Isotope Separator On Line (ISOL) of $M/\Delta M = 20000$ [29] for subsequent postacceleration. For this Day-one experiment, the ^{20}Na source was produced via the ^{24}Mg(p, αn)^{20}Na reaction with 100-MeV proton beam bombarding a MgO target. The MgO target is about 10 cm in thickness comprising of a stack of MgO slices, each with a thickness of about 2 mm. To facilitate the effusion of neutral ^{20}Na atoms out of their production lattices, each MgO slice was made into a microporous structure, and about 1/4 of each slice was deliberately cut off to form a diffusion volume in the target oven of cylindric tantalum tube. A surface ionization source was used to extract ^{20}Na ions with a working temperature of about 1500 °C. The design and manipulation of the MgO target and surface ionization source assembly is similar to the one described in Ref. [30]. After careful optimization of the working condition, a pure ^{20}Na ISOL beam of about 1×10^5 pps was reached with a 5-μA proton primary beam; the overall efficiency is comparable with the one reported in Ref. [31].

The experimental setup for the β decay of ^{20}Na is shown in Fig. 1. The ^{20}Na ISOL beam of 100 keV was implanted into a 3-μ-thick aluminum collection foil. The aluminum foil was situated in the center of a compact silicon box, which was formed by five pieces of multiguard silicon quadrant (MSQ) of 1 mm thick to measure the β particles. At the upstream, two pieces of double-sided silicon strip detector (DSSD) were installed 10 cm from the collection foil to measure the β-delayed α particles. Each DSSD was backed by an MSQ detector to reject the β summing events in the α particle spectrum. The DSSD has a thickness of about 70 μ with a very thin dead layer of only 100 nm to facilitate the detection of low-energy α particles. Two HPGe detectors, each with a relative efficiency of 175%, were installed in two cylindric flanges at angles of $\pm 90^\circ$ with respect to the beam direction to measure the γ rays. The absolute efficiency of HPGe detectors was

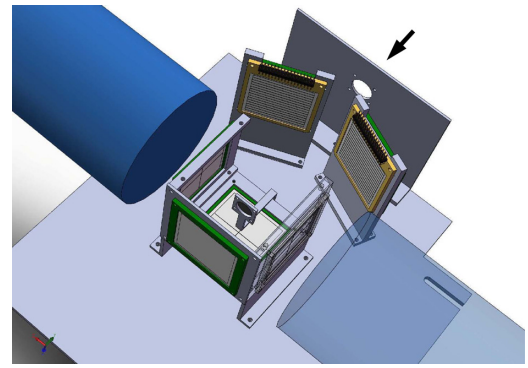

FIG. 1. Experimental setup for the β decay of ^{20}Na. The simultaneous measurement of β, α, and γ transitions from the ^{20}Na decay is realized by using five pieces of MSQ, two pieces of DSSD and two HPGe detectors, respectively. The top MSQ is removed to show the collection foil.

determined in a combined way as following. Standard sources of ^{152}Eu and ^{56}Co were used to determine the absolute efficiencies of γ rays up to about 3.5 MeV. The extrapolation to high-energy γ rays was realized by GEANT4 [32] simulation with the experimental geometry and the detector parameters. To do the simulation, one needs to know the relative detection efficiency curve up to high-energy region. This was done by measuring the well-known resonance in the ^{27}Al(p, γ)^{28}Si reaction at $E_p = 293$ keV [33] with the same HPGe detectors in several different distances. The implantation rate of ^{20}Na was controlled to about 1.5×10^4 pps throughout the experiment. About 4.5×10^9 ^{20}Na nuclei in total were implanted into the collection foil.

The α and γ singles spectrum from the β decay of ^{20}Na is shown in Fig. 2. The energy calibration of the β-delayed α singles spectrum was realized by using the well-determined α-particle lines [26], with the correction of energy-loss nonlinearity of α particle in the aluminum foil and the dead layer of DSSD. In addition to the 1634 keV $2_1^+ \rightarrow 0_{gs}^+$ transition and the 3334 keV $2^- \rightarrow 2_1^+$ transition in ^{20}Ne, five groups of high-energy γ lines, each includes the full-energy peak and single- and double-escape peaks are observed with good resolution as shown in Figs. 2(b) and 2(c), respectively. The 11262.3-keV 1^+ state is known with high precision from the ^{16}O(α, γ)^{20}Ne reaction [34] and the ^{20}Ne(γ, γ') photon scattering [35], the 11258.9(1.9)-keV γ transition is thus used for the energy calibration of γ singels spectrum. The intensity of γ rays is determined relative to that of the 1634-keV transition, while the latter is deduced to be 79.6(2.5)% per 100 decays of ^{20}Na from the net counts $N_\gamma(1634)$ by the following relation:

$$I_\gamma(1634) = \frac{N_\gamma(1634)}{N_\gamma(1634) + N_\gamma(11259) + N_\alpha(\text{total})}. \quad (1)$$

The total α-particle emission probability I_α(total) is deduced to be 20.3(6)% from the total α counts N_α(total) by the similar relation.

To explore the exotic β-γ-α decay sequences of ^{20}Na, an α-γ matrix was constructed taking all α-γ coincidence events

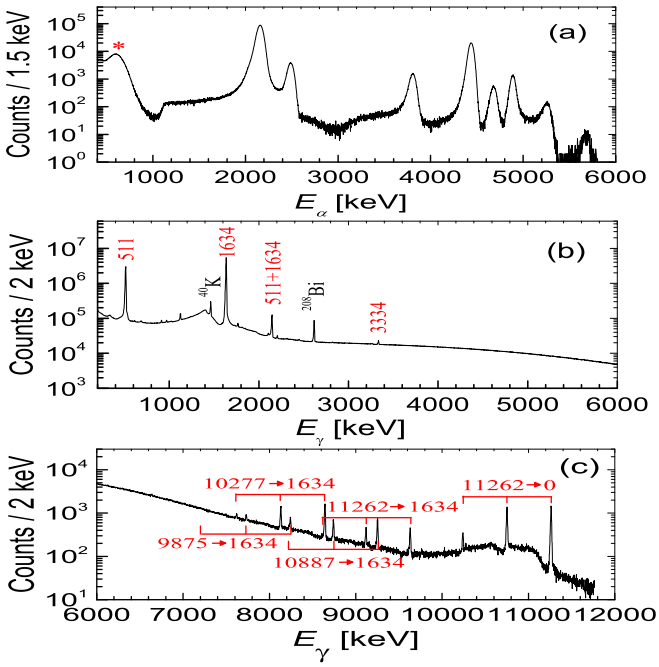

FIG. 2. α and γ singles spectrum of ^{20}Na decay. The peak in (a) labeled by an asterisk is dominated by ^{16}O recoils.

within 140 ns, as shown in Fig. 3. Since the readout energy of an α particle event by the front (E_f) and back sides (E_b) of DSSD follows diagonal relation, a criterion of $|E_f - E_b| <$ 140 keV was introduced to remove the $\alpha - \gamma$ coincidence events caused by the cross-talk effect of DSSD. The α gated γ spectra were projected at different α particle energy intervals from the α-γ matrix, as shown in Fig. 4. Two γ lines are seen in Fig. 4(a) at 4252 and 4655 keV, which coincide with the 9875 $\rightarrow$ 5621 keV and 10277 $\rightarrow$ 5621 keV transitions in ^{20}Ne, respectively. From the 4252- and 4655-keV γ gated α spectrum, $E_\alpha = 710(10)$ keV is obtained that agrees with the recently observed 714(4) keV α particle line emitted from the 5621-keV 3^- state in ^{20}Ne [26]. A γ line at 6130 keV is seen in Fig. 4(b), which is the $3^- \rightarrow 0^+_{gs}$ transition in ^{16}0. The 6130-keV γ gated α spectrum gives $E_\alpha = 1204(35)$ keV. The coincidence events are thus due to a β-α-γ sequence

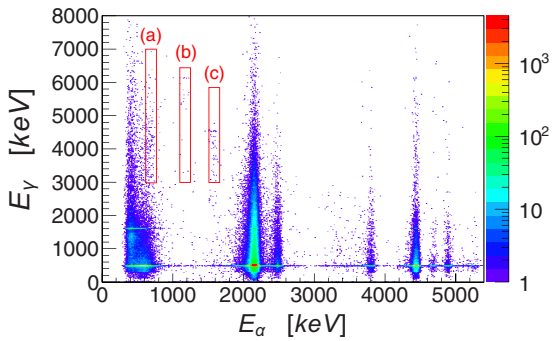

FIG. 3. Two-dimensional α-γ coincidence spectrum of ^{20}Na decay. The gates used for the projection on E_γ are indicated by rectangles.

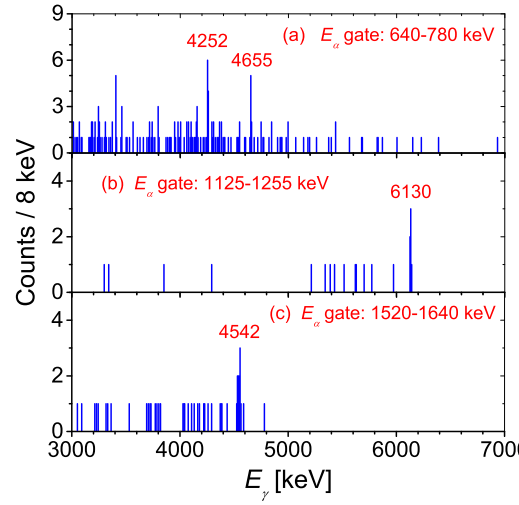

FIG. 4. γ spectra projected from the α-γ matrix with different α particle energy gates. See text for details.

through a 12367-keV ^{20}Ne level to the 6130-keV 3^- state in ^{16}0. A 4542-keV γ line is observed in Fig. 4(c), which is the 11262 $\rightarrow$ 6720-keV transition in ^{20}Ne. $E_\alpha = 1590(30)$ keV is obtained from the 4542-keV γ gated α spectrum, which agrees with a known 1589(5)-keV α particle line originated from the 6720-keV 0^+ state in ^{20}Ne.

A decay scheme of ^{20}Na is shown in Fig. 5 based on the γ and α lines and the α-γ coincidence observed in the present work. Three β-γ-α exotic decay sequences in ^{20}Na are shown in Fig. 5, their intensities are listed in Table I in comparison with the recently reported α particle intensities [26]. Two γ transitions deexciting from the 10277-keV IAS and 9875-keV 3^+ state to the 5621-keV level in ^{20}Ne, respectively, contribute to the α particle intensity observed at $E_\alpha = 714$ keV [26]. After subtraction, the direct β feeding has an upper limit (1σ) of 0.0029%, which corresponds to a lower limit of $\log ft >$ 8.5. For the 5788-keV 1^- level, no γ line is observed in coincidence with the $E_\alpha = 847$-keV region and the intensity of 847-keV α particle line [26] is taken for direct β feeding. The 5621-keV 3^- level and 5788-keV 1^- level have similar direct β feedings and $\log ft$ values, which are consistent with the first forbidden β transition.

The energy levels of ^{20}Ne populated in the β decay of ^{20}Na are listed in Table II. For the 1^+, 2^+, and 3^+ states in ^{20}Ne, the $\log ft$ values are in the range of 3.8 to 6.3 that generally agree with those expected for allowed GT transitions. The 8770(50)-keV 2^+ state in ^{20}Ne is known to have an α particle width of about 700 keV [26], its α particle intensity and $\log ft$ value are difficult to evaluate precisely due to an intense α peak centered at 3807 keV. For the 10277-keV IAS in ^{20}Ne, the superallowed Fermi transition is indicated by a $\log ft$ value of 3.48. For the 12367-keV state, the low $\log ft$ value indicates an allowed GT transition, which contains 12.5(5.6)% of electron capture branch according to calculation. Since a 2^+ $T = 0$ ^{20}Ne unbound level would decay dominantly to the ground state of ^{16}O, the 12367-keV state has to be of 1^+ or 3^+. We check the literature and find a reported 1^+ state at 12367(15) keV from the angular distribution of

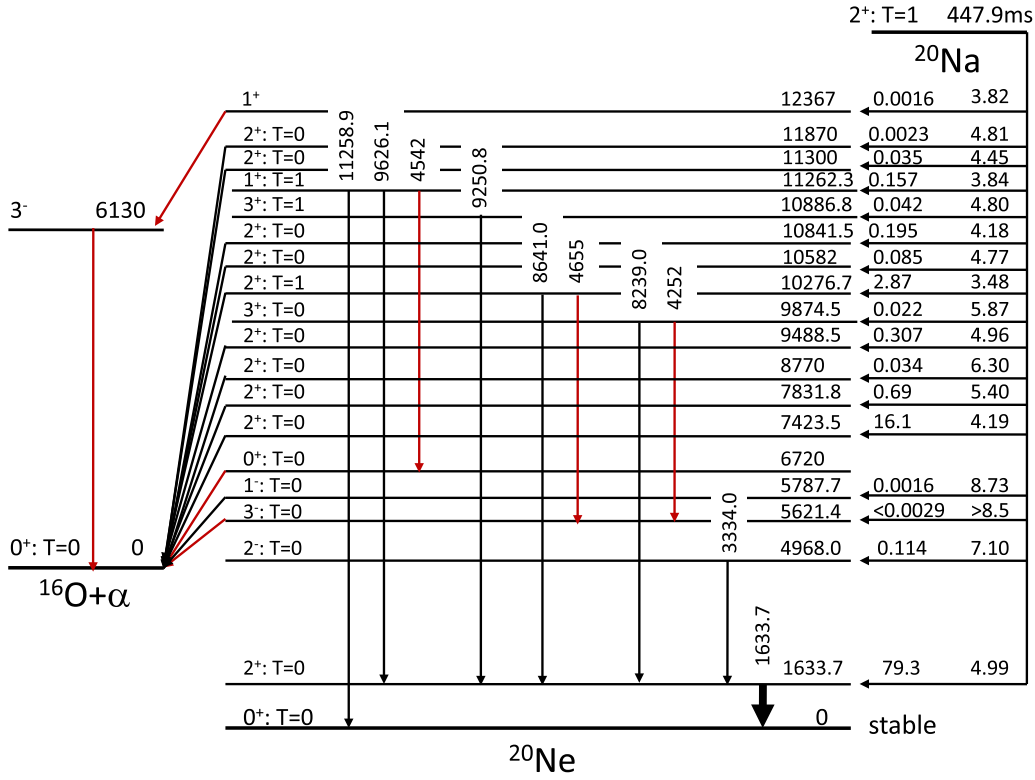

FIG. 5. Decay scheme of ^{20}Na. The newly discovered exotic decay sequences are shown with red arrows. The ^{20}Ne states are labeled by excitation energy in keV, β branching ratio, and logft value on the right side.

^{19}F(^{3}He, d)^{20}Ne reaction [38], which has not been included in the compilation. This should also correspond to the suggested new 1^+ state at 12389 keV based on an α particle line of 1220(30) keV in Ref. [26]. The transition strength $B(F)$ and $B(GT)$ are related to the experimental ft by

$$ft = \frac{K}{g_V^2 B(F) + g_A^2 B(GT)}, \tag{2}$$

where $K/g_V^2 = 6144.2(1.6)$ s and $g_A/g_V = -1.2694(28)$ [12]. The $B(F)$ and $B(GT)$ are accordingly deduced as listed in Table II.

The β decay of ^{20}Na is calculated in the *sd* shell-model space with USDB interaction [39,40] for the charge independent part plus the Coulomb, charge-dependent, and charge-asymmetric nuclear Hamiltonian for the *sd* shell [41]. As listed in Table II, five 2^+ states, two 3^+ and two 1^+ states in ^{20}Ne are predicted with β transition strengths from the ^{20}Na decay, the calculated $B(GT)$ values scaled with a quenching factor of $q^2_{(GT)} = 0.60$ [40] agree well with the experimental ones. For the 10277-keV IAS in ^{20}Ne, the calculated total β transition strength has $B(GT) = 0.093$ and $B(F) = 1.994$. The reduction in $B(F)$ is due to isospin mixing with other 2^+ $T = 0$ states, this isospin mixing can account for the observed isospin-forbidden α decay of the IAS. The calculated γ decay width of the IAS is 3.95 eV compared to 4.58 ± 0.51 eV observed in the ^{16}O(α, γ)^{20}Ne reaction [42]. If the 2^+ IAS had pure $T = 1$, then the α decay is forbidden. However, the IAS is observed to have an α decay width of 116(20) eV from another ^{16}O(α, γ)^{20}Ne reaction [43]. The calculation predicts that 2^+ $T = 0$ states 493 and 800 keV above the IAS mix with the IAS with isospin-mixing matrix elements of 17 and 28 keV, respectively. If we associate these with states at 10 582 and 10 842 keV (305 and 565 keV above the IAS, respectively), they would have to have allowed α decay widths that total of about 150 keV in order to give 116 eV for the IAS. There are four 2^+ $T = 0$ states in the

TABLE I. Exotic decay sequences of ^{20}Na observed in this work by γ-α coincidence.

E_γ (keV)	E_α (keV)	Decay sequence	I(%)[a]	E_α in Ref. [26]	I(%) in Ref. [26]
4252 (5)	710 (10)	^{20}Ne(9875) → ^{20}Ne(5621) → ^{16}O$_{gs}$	0.0018 (6)	714 (4)	0.0024 (3)[b]
4542 (5)	1590 (30)	^{20}Ne(11262) → ^{20}Ne(6720) → ^{16}O$_{gs}$	0.0024 (7)	1589 (5)	0.0013 (2)
4655 (4)	710 (10)	^{20}Ne(10277) → ^{20}Ne(5621) → ^{16}O$_{gs}$	0.0016 (6)	714 (4)	0.0021 (3)[b]
6130 (4)	1204 (35)	^{20}Ne(12367) → ^{16}O(6130) → ^{16}O$_{gs}$	0.0016 (7)	1220 (30)	0.0010 (3)

[a]Absolute intensity per 100 ^{20}Na decay.
[b]An intensity of 0.0045% is reported for $E_\alpha = 714$ keV [26], it is split here for comparison.

TABLE II. Levels in ^{20}Ne populated in the β decay of ^{20}Na. Logft values are calculated with $Q_\beta = 13892.5(11)$ keV [36] and $T_{1/2} = 447.9(23)$ ms [37]. Shell-model calculation in the *sd* shell-model space is listed for comparison.

Present experiment					Shell model			
E_x (keV)	I^π	β feeding (%)	logft	$B_{F/GT}$	E_x (keV)	B_{GT}[a]	$B(F)$	Γ_γ (eV)
0.0	0^+							
1633.7 (2)[b]	2^+	79.3(25)	4.99	0.039	1738	0.035	0.00001	0.0006
4968.0 (7)[b]	2^-	0.114(8)	7.10					
5621.4 (17)[c]	3^-	<0.0029	>8.5					
5787.7 (26)[c]	1^-	0.0016(5)[d]	8.73					
6720 (5)[b]	0^+				6698			0.021
7423.5 (18)	2^+	16.1(6)	4.19	0.245	7533	0.182	0.00044	0.020
7831.8 (23)	2^+	0.69(3)	5.40	0.015				
8770 (50)	2^+	0.034(8)	6.30	0.002				
9488.5 (22)	2^+	0.307(18)	4.96	0.042				
9874.5 (21)[b]	3^+	0.022(6)	5.87	0.005	10419	0.0005		0.017
10276.7 (20)[b]	2^+	2.87(12)	3.48	2.044	9947	0.093	1.994	3.947
10582 (3)	2^+	0.085(4)	4.77	0.065	10440	0.201	0.0024	0.019
10841.5 (22)	2^+	0.195(8)	4.18	0.253	10747	0.417	0.0025	0.110
10886.8 (22)[b]	3^+	0.042(4)	4.80	0.060	10538	0.086		3.782
11262.3 (19)[b]	1^+	0.157(8)	3.84	0.552	11135	0.510		18.54
11300 (10)	2^+	0.035(2)	4.45	0.135				
11870 (50)	2^+	0.0023(1)	4.81	0.059				
12367 (35)	1^+	0.0016(7)	3.82	0.577	12573	0.211		0.626

[a]A quenching factor of $q^2_{(GT)} = 0.60$ [40] is multiplied.
[b]Determined by γ transitions from this work. The remaining excitation energies are determined by α particle lines or otherwise labeled.
[c]From compilation in Ref. [24].
[d]From Ref. [26].

region from 10.6 to 11.9 MeV with α widths to the ^{16}O ground state ranging from 13 to 250 keV [24,26]. Mixing with these states may contribute to the α decay width of the IAS, but we are unable to calculate their contributions since they lie outside of the *sd* shell-model space. The isospin-mixing matrix element with the first excited 2^+ $T = 0$ state is 15 keV. The α decay width of this state (at the energy of the IAS) would have to be about 18 MeV to account for the 116-eV α decay width of the IAS. This is much larger than the estimated ^{16}O + α cluster decay width of about 1 MeV.

In conclusion, the β decay of ^{20}Na is reinvestigated in the Day-one experiment at BRIF with an intense pure ^{20}Na ISOL beam and challenging α-γ coincidence analysis. Three exotic β-γ-α decay sequences in ^{20}Na are successfully observed, which is the first case in its type, thus expands the rare decay modes discovered in β decay. The observed β-γ-α decay sequences are essential in determining the direct β feedings and logft values to the low-lying α-emitting states in ^{20}Ne. Although the α decay widths for these states have not yet been calculated, the experimental β transition strengths to the 1^+, 2^+, and 3^+ states in ^{20}Ne can be well accounted for by using *sd* shell-model space interactions.

The authors thank the technical staff for their efforts to deliver the ^{20}Na ISOL beam. This work is supported by the National Key Research and Development Project under Grant No. 2016YFA0400502; the Continuous Basic Scientific Research Project under Grant No. WDJC-2019-13; the National Natural Science Foundation of China under Grants No. 11875322, No. 11327508, No. 11490560, No. U1867211, and No. U1867214; NSF Grant No. PHY-1811855; and the CUSTIPEN (China-U.S. Theory Institute for Physics with Exotic Nuclei) funded by the US Department of Energy, Office of Science, under Grant No. DE-SC0009971.

[1] F. Osterfeld, Rev. Mod. Phys. **64**, 491 (1992).
[2] Y. Fujita, B. Rubio, and W. Gelletly, Prog. Part. Nucl. Phys. **66**, 549 (2011).
[3] K. Langanke and G. Martínez-Pinedo, Rev. Mod. Phys. **75**, 819 (2003).
[4] S. Hofmann, W. Reisdorf, G. Münzenberg, F. P. Heßberger, J. R. H. Schneider, and P. Armbruster, Z. Phys. A **305**, 111 (1982).
[5] O. Klepper *et al.*, Z. Phys. A **305**, 125 (1982).
[6] J. Giovinazzo *et al.*, Phys. Rev. Lett. **89**, 102501 (2002).
[7] M. Pfützner *et al.*, Eur. Phys. J. A **14**, 279 (2002).
[8] M. D. Cable, J. Honkanen, R. F. Parry, S. H. Zhou, Z. Y. Zhou, and J. Cerny, Phys. Rev. Lett. **50**, 404 (1983).
[9] H. O. U. Fynbo *et al.*, Nature **433**, 136 (2005).
[10] D. E. M. Hoff *et al.*, Nature **580**, 52 (2020).

[11] B. Blank and M. J. G. Borge, Prog. Part. Nucl. Phys. **60**, 403 (2008).
[12] M. Pfützner, M. Karny, L. V. Grigorenko, and K. Riisager, Rev. Mod. Phys. **84**, 567 (2012).
[13] C. Qi, R. Liotta, and R. Wyss, Prog. Part. Nucl. Phys. **105**, 214 (2019).
[14] J. Su *et al.*, Phys. Lett. B **756**, 323 (2016), and references therein.
[15] M. Bhattacharya *et al.*, Phys. Rev. C **77**, 065503 (2008).
[16] S. E. A. Orrigo *et al.*, Phys. Rev. Lett. **112**, 222501 (2014).
[17] R. D. Macfarlane and A. Siivola, Nucl. Phys. **59**, 168 (1964).
[18] D. F. Torgerson, K. Wien, Y. Fares, N. S. Oakey, R. D. Macfarlane, and W. A. Lanford, Phys. Rev. C **8**, 161 (1973).
[19] W. X. Huang *et al.*, Sci. China A **40**, 638 (1997).
[20] P. D. Ingalls, Phys. Rev. C **14**, 254 (1976).
[21] N. S. Oakey and R. D. Macfarlane, Phys. Rev. Lett. **25**, 170 (1970).
[22] S. J. Freedman, R. D. Cousins, Jr., C. A. Gagliardi, G. T. Garvey, and J. F. Greenhalgh, Phys. Lett. B **67**, 165 (1977).
[23] E. T. H. Clifford *et al.*, Nucl. Phys. A **493**, 293 (1989).
[24] D. R. Tilley, C. M. Cheves, J. H. Kelley, S. Raman, and H. R. Weller, Nucl. Phys. A **636**, 249 (1998).
[25] J. D. Pearson, E. Almqvist, and J. A. Kuehner, Can. J. Phys. **42**, 489 (1964).
[26] K. L. Laursen, O. S. Kirsebom, H. O. U. Fynbo, A. Jokinen, M. Madurga, K. Riisager, A. Saastamoinen, O. Tengblad, and J. Äystö, Eur. Phys. J. A **49**, 79 (2013).
[27] W. P. Liu *et al.*, Sci. China Phys. Mech. Astron. **54**, s14 (2011).
[28] T. J. Zhang *et al.*, Nucl. Instrum. Methods B **266**, 4117 (2008).
[29] B. Q. Cui *et al.*, Nucl. Instrum. Methods B **266**, 4113 (2008).
[30] B. Tang *et al.*, Nucl. Instrum. Methods B **463**, 154 (2020).
[31] M. Dombsky *et al.*, Nucl. Instrum. Methods B **264**, 117 (2007).
[32] J. Allison *et al.*, Nucl. Instrum. Methods A **835**, 186 (2016).
[33] M. A. Meyer, I. Venter, and D. Reitmann, Nucl. Phys. A **250**, 235 (1975).
[34] L. K. Fifield, W. N. Catford, S. H. Chew, E. F. Garman, D. M. Pringle, K. W. Allen, and J. Lowe, Nucl. Phys. A **394**, 1 (1983).
[35] U. E. P. Berg, K. Ackermann, K. Bangert, R. Stock, and K. Wienhard, Phys. Rev. C **27**, 2981 (1983).
[36] M. Wang, G. Audi, F. G. Kondev, W. J. Huang, S. Naimi, and X. Xu, Chin. Phys. C **41**, 030003 (2017).
[37] G. Audi, F. G. Kondev, M. Wang, W. J. Huang, and S. Naimi, Chin. Phys. C **41**, 030001 (2017).
[38] R. R. Betts, H. T. Fortune, and R. Middleton, Phys. Rev. C **11**, 19 (1975).
[39] B. A. Brown and W. A. Richter, Phys. Rev. C **74**, 034315 (2006).
[40] W. A. Richter, S. Mkhize, and B. A. Brown, Phys. Rev. C **78**, 064302 (2008).
[41] W. E. Ormand and B. A. Brown, Nucl. Phys. A **491**, 1 (1989).
[42] L. K. Fifield, F. P. Calaprice, C. H. Zimmerman, M. J. Hurst, A. Pakkanen, T. J. M. Symons, F. Watt, and K. W. Allen, Nucl. Phys. A **288**, 57 (1977).
[43] P. D. Ingalls, Nucl. Phys. A **265**, 93 (1976).